ELSEVIER

Journal of Power Sources 110 (2002) 96–106

JOURNAL OF POWER SOURCES

www.elsevier.com/locate/jpowsour

An electrochemical technique for state of charge (SOC) probing of positive lead–acid battery plates

Paul J. Blood[a], Sotiris Sotiropoulos[b,*]

[a]*School of Chemical, Environmental and Mining Engineering, The University of Nottingham, University Park, Nottingham NG7 2RD, UK*
[b]*Physical Chemistry Laboratory, Department of Chemistry, Aristotle University of Thessaloniki, Thessaloniki 54124, Greece*

Received 12 December 2001; received in revised form 26 March 2002; accepted 3 April 2002

Abstract

Electrochemical experiments that intend to characterise the state of charge (SOC) of lead–acid battery positive plates are presented. These experiments are designed for potential battery plate production quality control and in situ monitoring of battery condition. A small size probe, consisting of a counter and a reference electrode encased in a glass body ending to a fine aperture tip and pressed onto the specimen, was used to apply cathodic galvanostatic pulses on positive plate battery samples. Although this probe arrangement is similar to that of a coulometric thickness gauge, the porous nature of the battery plate results eventually in full discharge of the entire specimen. However, during the initial stages of specimen discharge using the contact probe, a potential arrest was observed for fully charged and partially discharged samples and it was attributed to the time needed for the thickness of a $PbSO_4$ film formed during discharge and the corresponding resistance under the probe's tip to reach a critical value for the discharge to spread to the rest of the sample. The duration of this potential arrest was found to be related to the positive plate's SOC indicating the possibility of using the technique in positive plate quality control or in situ monitoring.

Keywords: Lead–acid batteries; State of charge sensors; Coulometric gauge

1. Introduction

Rechargeable batteries are receiving increasing attention as the demand for environmentally clean energy sources expands. Traditional applications include starting, lighting and ignition of automobiles, electric traction and uninterruptible power supplies used in telecommunications, substations, chemical plants and nuclear installations [1–5].

The emerging electric vehicle technology aiming to the development of fuel-cell/battery hybrid electric cars [6] has further stimulated research into rechargeable batteries. Despite the emergence of new battery types and fuel-cells, the lead–acid battery is still the most attractive option from an economic point of view and is expected to dominate the above mentioned applications for the foreseeable future.

The electrochemistry of both positive and negative plate electrodes and lead–acid battery grids has been thoroughly studied in the past and manufacturing of the main components of the various types that are commercially available is a mature technology [1–3]. However, there is ongoing research into new charging and monitoring circuits and strategies to improve battery lifetime and performance. To that direction, a useful parameter in evaluating the battery's state of health and optimising its utilisation is the state of charge (SOC), defined as the ratio of remaining available capacity (at a certain point of its lifetime) to the maximum attainable capacity (under certain discharge conditions).

Simple monitoring of the voltage difference across the battery terminals, although in principle the most direct method for SOC estimation, is not very useful in early diagnosis of battery failure since significant voltage changes during discharge only occur abruptly and just before the battery's life end. Therefore, other techniques which follow phenomena directly or indirectly linked to the SOC have been developed as diagnostic tests: specific gravity tests and acid stratification monitoring using simple or optical hydrometers [7,8] or laser interferometry [9,10], pressure transducers to detect gassing during charging [11], humidity sensors [12], electrochemical noise monitoring for early detection of imminent failure [5], ac impedance techniques [13–15] or internal resistance measurements by dc current-interrupt techniques [16]. The first four of these techniques require the incorporation of additional devices in the cell body and provide indirect information about the SOC. From the electrochemical techniques, ac impedance

* Corresponding author. Tel.: +30-310-997742; fax: +30-310-443922.
E-mail addresses: eczss@chem.auth.gr, eczss@otenet.gr (S. Sotiropoulos).

0378-7753/02/$ – see front matter
PII: S0378-7753(02)00231-8

requires careful choice of the cell parameter to be correlated with SOC and there is some disagreement on its predictive efficiency for lead–acid batteries [14,15]. Finally, changes in the internal cell resistance by the current-interrupt technique are only pronounced close to the end of deep discharge [16]. There is therefore, scope for research into new techniques that could be developed into SOC probes either for individual battery plate quality control or for in situ cell monitoring.

Coulometric determination of metal oxides on metallic substrates by controlled electrochemical reduction of small specimens has long been established as a technique to quantify and characterise oxidised metal films such as tin oxides on Sn or cuprous/cupric films on Cu [17,18]. The total discharge of PbO_2 of positive lead–acid battery plate specimens as a means of positive plate quality control during production [1] can also be viewed as a kind of coulometric determination whereas the constant current reduction of Pb grid oxidation products has recently been proposed as a means of electrometric evaluation of lead alloy corrosion [19]. At the same time coulometric thickness gauges (based on the electrochemical oxidation of metals) have long been established as standard probes for the determination of metal coating thickness on metallic and non-metallic substrates [20] and a number of commercial instruments are available (see for example the Couloscope® CMS by Fischer Instrumentation Ltd. [21]). With these probes, rather than electrochemically de-plating-destroying the entire specimen, the measurement is taken over an area as small as possible (e.g. of a 0.6 mm diameter for Couloscope® CMS) by a miniature electrochemical cell (containing the electrolyte and the counter electrode) sealed onto the substrate by an O-ring.

This work is investigating the possibility of using a small probe based on the same general principle of the coulometric thickness gauge, to evaluate the SOC of positive lead–acid battery plates by local (or at least partial) discharge-reduction of their PbO_2 content. There is however, a marked difference between the situation at a metal thickness coulometric gauge and any local probe that might be used onto battery plates: in the former case electrochemistry is strictly restricted in the area defined by the opening of the probe's cell which is sealed on the non-porous coating and contains the electrolyte and when this area is de-plated a sharp change in the potential occurs; in the latter case, due to the porous nature of battery plate specimens (and the existence of electrolyte over the entire battery plate if the probe is to be used in situ after miniaturisation) the electric field is expected to spread to the entire specimen or plate. Nevertheless the uneven current distribution during discharge by a small probe (counter electrode, reference electrode and electrolyte) contained in an insulating body and pressed onto a positive plate specimen is likely to alter the typical potential-time discharge curve and introduce additional features.

The aim of this work is to correlate the features of the constant current discharge of positive battery plate specimens obtained with the help of a small electrode probe, with the SOC of the battery specimen and set the principles of using this technique for the development of coulometric probes for battery plate quality control during production or (with appropriate miniaturisation) in situ determination of the SOC of positive plates during battery operation.

2. Experimental

2.1. Electrochemical cells and equipment

The two modifications of the cell used for the normal discharge of the entire positive plate specimen (referred to as total discharge hereafter) and for discharge via the coulometric small probe (referred to as probe discharge or contact mode discharge hereafter) are presented in Fig. 1(a) and (b). In both cases, the test cell consisted of a Teflon® tube (2 cm i.d.) having a rim at one end and pressed onto a Teflon® base plate (bottom plate in Fig. 1). The square positive plate specimen ($1.7\ cm \times 1.7\ cm = 2.89\ cm^2$) was glued with carbon conductive cement (LEIT-C, Electron Beam Sciences Inc.) onto a Pb foil square of the same dimensions ending to a strip and acting as a current collector (0.25 mm thick, 99.95%, Goodfellow Ltd.). The battery plate specimen electrode was placed on the base Teflon® plate with the battery specimen inside the Teflon® tube and its strip passing through a groove of its rim. The tube and bottom plate were held tightly together and sealed by another ring-shaped Teflon® plate and a rubber gasket, both lying on the tube rim and screwed firmly on the bottom plate. The tubular cell was filled with a 5 M degassed H_2SO_4 solution.

In the case of total specimen discharge (Fig. 1(a)) a 20 cm long Pt coil served as the counter electrode (0.5 mm diameter Pt wire, 99.99%, Goodfellow Ltd.) and a saturated calomel electrode (SCE, EG&G Perkin-Elmer Inc.) or a saturated mercury sulphate electrode (SMSE, Cumbria Instruments Ltd.) equipped with a plastic body bridge ending to a Vycor® tip (EG&G Perkin-Elmer Inc.) were the reference electrodes used. No difference in results obtained with either electrode was observed and all potentials are given with respect to the SCE. The end of the reference electrode system tip was held at a fixed 1.2 cm distance from the battery plate specimen.

In the case of probe discharge experiments (Fig. 1(b)) the reference electrode bridge end tubing (3 mm o.d.) and a 5 cm long, 0.5 mm thick Pt coil (Goodfellow Ltd.) were packed inside a glass pipette of 4.5 mm i.d. which converged to a final aperture of 2.8 mm diameter ($0.06\ cm^2$). The glass pipette was filled with a 5 M degassed H_2SO_4 solution and pressed firmly onto the battery specimen. The tip of the reference electrode tubing was again at a fixed distance of 1.2 cm from the specimen.

2.2. Positive plate electrodes and chemicals

Positive lead–acid battery plates were taken from a UK6TN Hawker–Oldham tank starter battery. Each battery

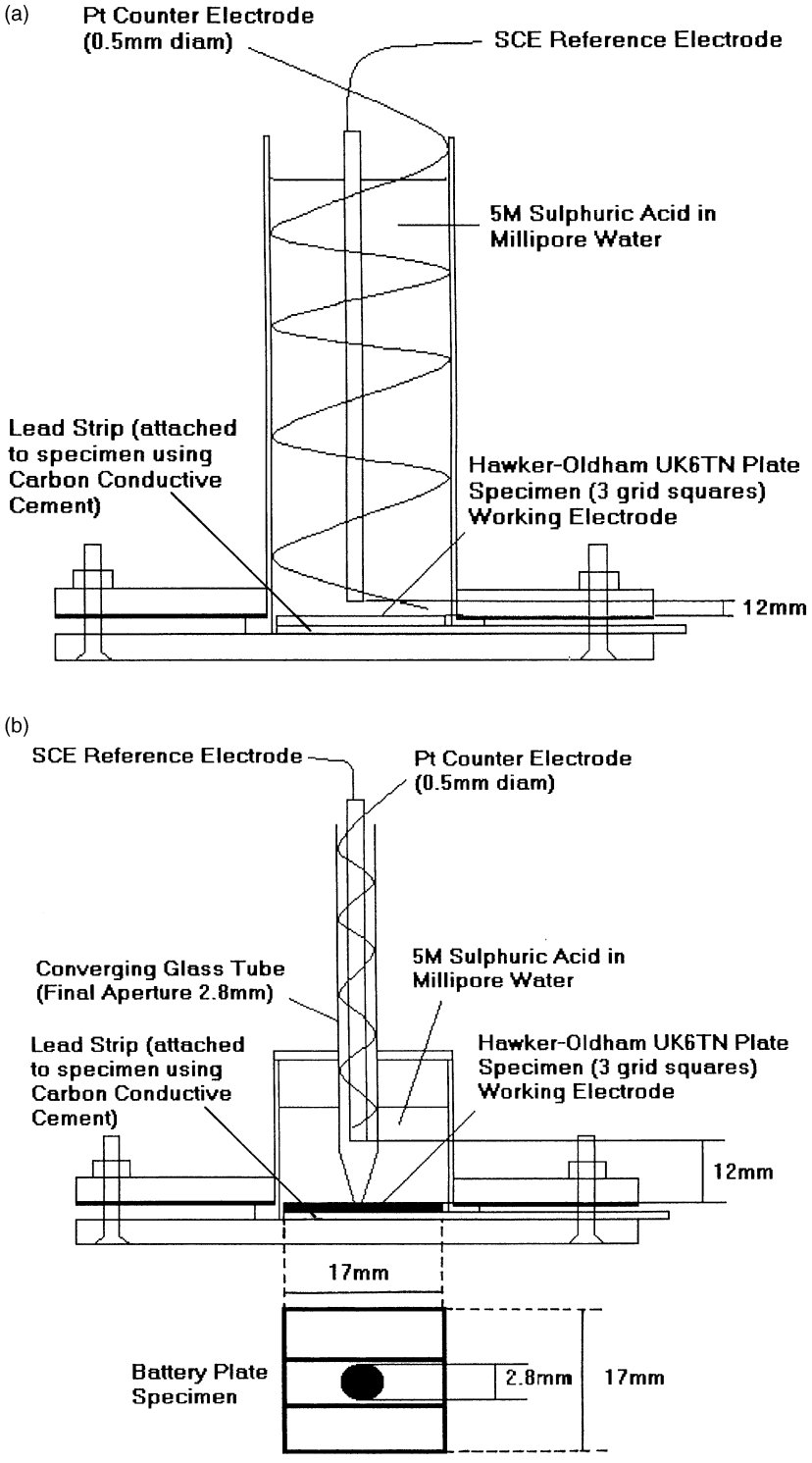

Fig. 1. (a) Electrochemical cell for positive plate specimen "total discharge". (b) Discharge probe and electrochemical cell arrangement for "probe discharge" tests.

plate had a nominal 8 Ah capacity at the 20 h rate. The grids had a 2.75% Sb content and the positive active material was determined by XRD to be 75% β-PbO_2 and 25% α-PbO_2. Plate thickness was in the 1.8–2 mm range as measured by a micrometer. Square specimens of an area $1.7\ \text{cm} \times 1.7\ \text{cm} = 2.89\ \text{cm}^2$ were cut off a plate (66 specimens to the plate) and had 1.52 g PbO_2 each corresponding to a theoretical capacity of 0.34 Ah or 1224 C each taking into account the value of 4.46 g PbO_2/Ah given in [1] (scaled up to an entire plate of 66

specimens this gives a theoretical capacity of 22.44 Ah for each plate which, together with the nominal 8 Ah capacity at the 20 h rate, results in a utilisation coefficient of 35.65% for that rate).

Sulphuric acid from Aldrich (double distilled, PPB/Teflon® grade) and deionised water from a Millipore® purification system were used for the preparation of electrolyte solutions.

3. Results and discussion

3.1. Discharge properties of positive plate battery specimens

The positive plate battery specimens were first characterised with respect to their capacity, C, utilisation and energetic coefficients, α and β ([1,22–24], see the following paragraph) and their average resistance R_{ave} [24], as a function of discharge rate.

Fig. 2(a) presents a set of potential, E versus time, t curves corresponding to deep discharge of the specimens in 5 M H_2SO_4 under galvanostatic control at a wide range of moderate to high current densities. The open circuit potential of the PbO_2 electrode was 1.53 V versus SCE (1.77 V versus SHE), and the end potential of the deep discharge, corresponding to the $PbSO_4$/Pb transformation was −0.65 V versus SCE (−0.39 V versus SHE) in accordance with the literature [1]. The additional potential plateau in the −0.2–0.5 V versus SCE range is usually attributed to a PbO_2/PbO intermediate transformation at the highly alkaline conditions prevailing under the initially formed $PbSO_4$ film [25,26]. This arrest is usually observed for moderate or high discharge rates and it is not very reproducible [1]. The deep discharge capacity of each specimen was determined up to an end potential of 0 V versus SCE. For the 27.68 mA cm^{-2} current density (curve E, 0.9 h rate), used for most of the subsequent total and local discharge experiments, a specimen capacity of 275.4 C was thus calculated corresponding to a low utilisation coefficient (ratio of experimental to maximum theoretical capacity) $\alpha = 22.5\%$ for this fast discharge rate.

The inset of Fig. 2(a) shows the variation of end-of-discharge time, t with current I in a log–log graph. The linearity of the plot and its slope (−1.44) are in complete agreement with Peukert's empirical equation [1]

$$I^n t = k \tag{1}$$

that holds for moderate to high discharge rates (n has a value of 1.3–1.4 for moderate rates and increases up to 2 at higher rates).

Fig. 2(b) presents a few low current density-long discharge E versus t curves. Its inset presents a plot of the logarithm of capacity C versus discharge current I. According to D'Alkaine et al. [23] this plot should be preferred at low discharge rates where Peukert's equation does not hold and instead the following empirical equation should be used:

$$\log C = mI + \log C_0 \tag{2}$$

where m is an empirical constant and C_0 the capacity at zero discharge rate; the latter is the maximum practical capacity that can be obtained from the active material of a plate of a given technology and is thus characteristic of the real electroactive area of the active material. The ratio of this maximum practical capacity to the theoretical capacity has been defined as the energetic coefficient, β, is independent of discharge rates and (for positive plates) from acid concentration too [23]; hence, it can be used to characterise a given plate production technology. From the intercept of the plot shown in the inset of Fig. 2(b) it follows that $C_0 = 728.6$ C and hence $\beta = 59.5\%$. Finally, from this set of slow discharge curves it is found that the utilisation coefficient at the 20 h rate (2.67 mA cm^{-2} for a single specimen) is $\alpha = 42.4\%$.

The average resistance R_{ave} of a specimen of a geometric area A at a given discharge extent corresponding to a charge of Q_d, is defined by [24]:

$$R_{ave}A = -\left(\frac{\partial E}{\partial i}\right)_{Q_d} \tag{3}$$

and can be determined by performing specimen discharge at different current densities, i, until a charge equal to Q_d has passed, measuring the corresponding potential and plotting it versus the current density. The minus sign in Eq. (3) is due to the reduction process taking place. Fig. 3 shows such a plot for potentials taken from the curves of Fig. 2 that correspond to points of a charge withdrawal equal to 20 C. These potentials are all located in the early part of the plateau in the E versus t curves. It follows that $R_{ave}A = 3.2\ \Omega\ cm^2$ (and $R_{ave} = 1.11\ \Omega$ for the specimen of 2.89 cm^2). This resistance is made up of the plate resistance R_{plate} (with a polarization part R_p and an ionic/electronic resistance through the plate part $R_{ion/el}$) and the uncompensated ionic resistance of the acidic solution between the specimen and the reference electrode tip, R_{acid}. The latter can be estimated from the specific conductivity, κ, of the 5 M H_2SO_4 which was measured as 0.65 S cm^{-1}, and the reference-specimen distance $l = 1.2$ cm to be $R_{acid}A = l/\kappa = 1.85\ \Omega\ cm^2$ ($R_{acid} = 0.64\ \Omega$); obviously, it also depends on the specific electrochemical cell arrangement and particularly on the shape of the electric field and the inter-electrode gaps. Hence, since $R_{ave} = R_{plate} + R_{acid}$, it follows that $R_{plate}A = 1.35\ \Omega\ cm^2$ and $R_{plate} = 0.47\ \Omega$. The Ohmic behaviour of the discharge over a wide current density range (reasonable linearity of the E versus I curve and R_{ave} constancy) are indicative of a discharge mechanism determined by ionic transfer through a solid state film [24,27]. The resistance values calculated earlier will be used in the interpretation of the total and local discharge experiments discussed in Section 3.3.

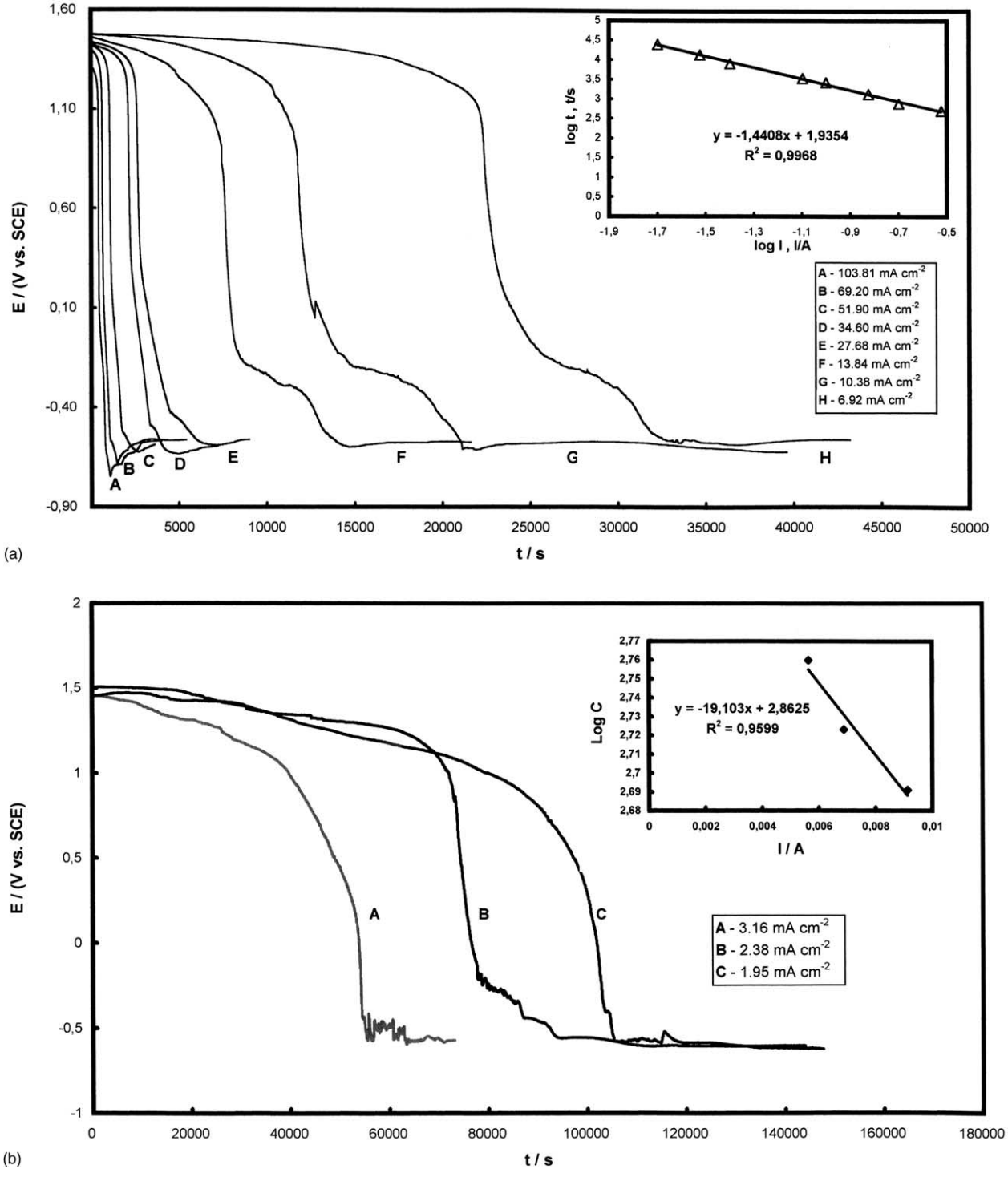

Fig. 2. (a) Positive plate specimen potential vs. time discharge curves at various moderate to high current densities; inset: Peukert equation plot. (b) Positive plate specimen potential vs. time discharge curves at various low current densities; insert: D'Alkaine's equation plot.

3.2. Correlation of duty-of-discharge of positive plate specimens with results of potential sweep and constant potential experiments

In order to produce positive battery plate specimens of different SOC, specimens were discharged at a current density of 27.68 mA cm^{-2} (0.085 A) for different time periods. The extent of specimen discharge or duty-of-discharge (DOD, defined as the ratio of discharged capacity to the maximum attainable capacity, thus related to SOC by DOD = 1 − SOC) was then estimated as the ratio of this time to the time needed for deep discharge which was taken as the time needed for the voltage to drop to 0 V versus SCE.

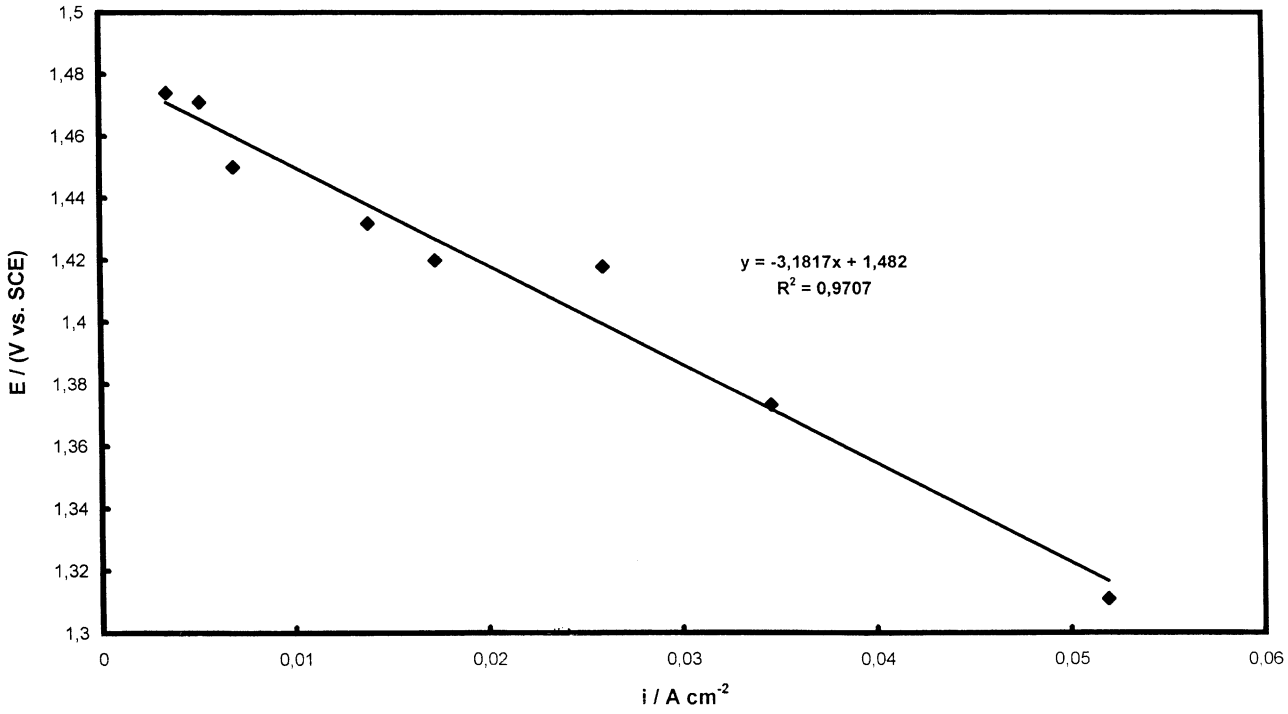

Fig. 3. Variation of positive plate specimen potential value, after the passage of 20 C at various discharge rates, with discharge current density.

To correlate the remaining available charge with the DOD of specimens thus produced, the latter were potentiostatically reduced at an overpotential $\eta = -0.3$ V from their rest potential. Fig. 4 shows the corresponding current density versus time curves and its inset the variation of remaining charge (calculated from the area underneath the curves) with prior DOD; a smooth variation is observed.

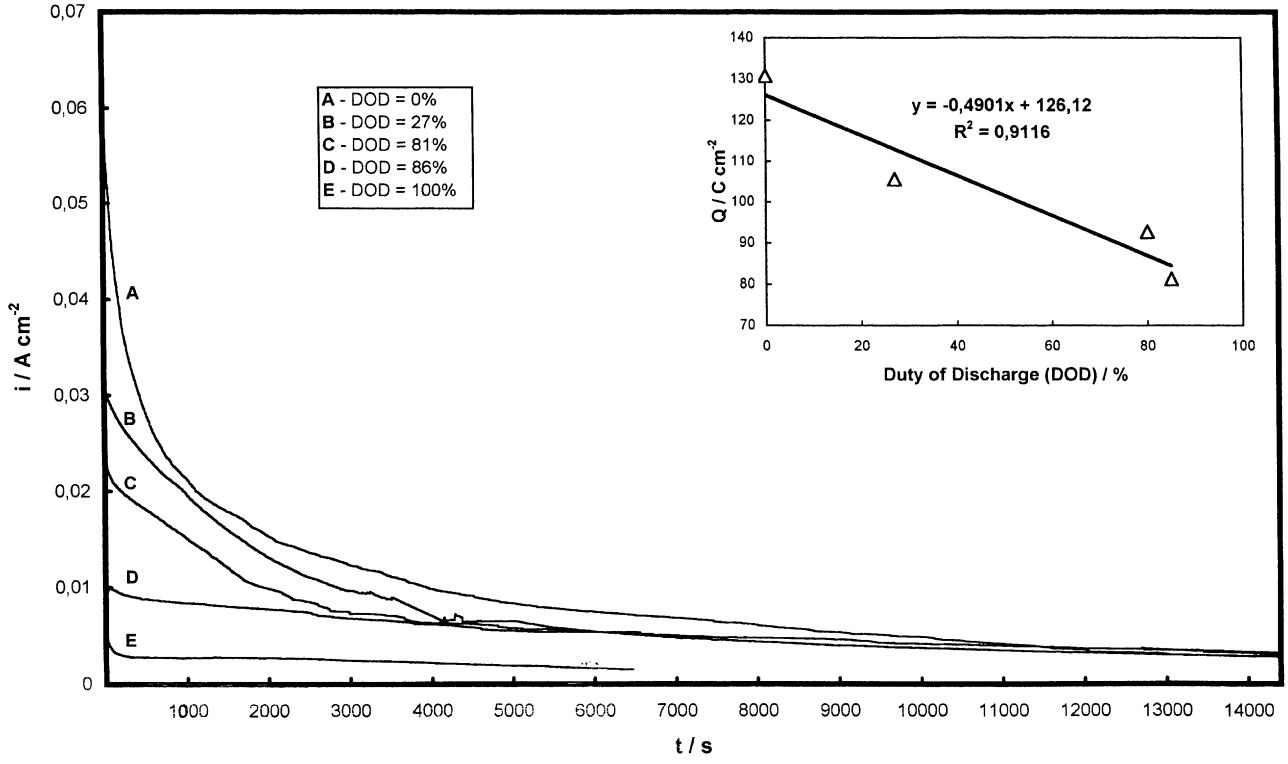

Fig. 4. Current density transients of positive plate specimens discharged at 0.085 A to various DOD levels, following potential steps −0.3 V with respect to their open circuit potential. Inset: variation of the charge passed during constant potential discharge with DOD.

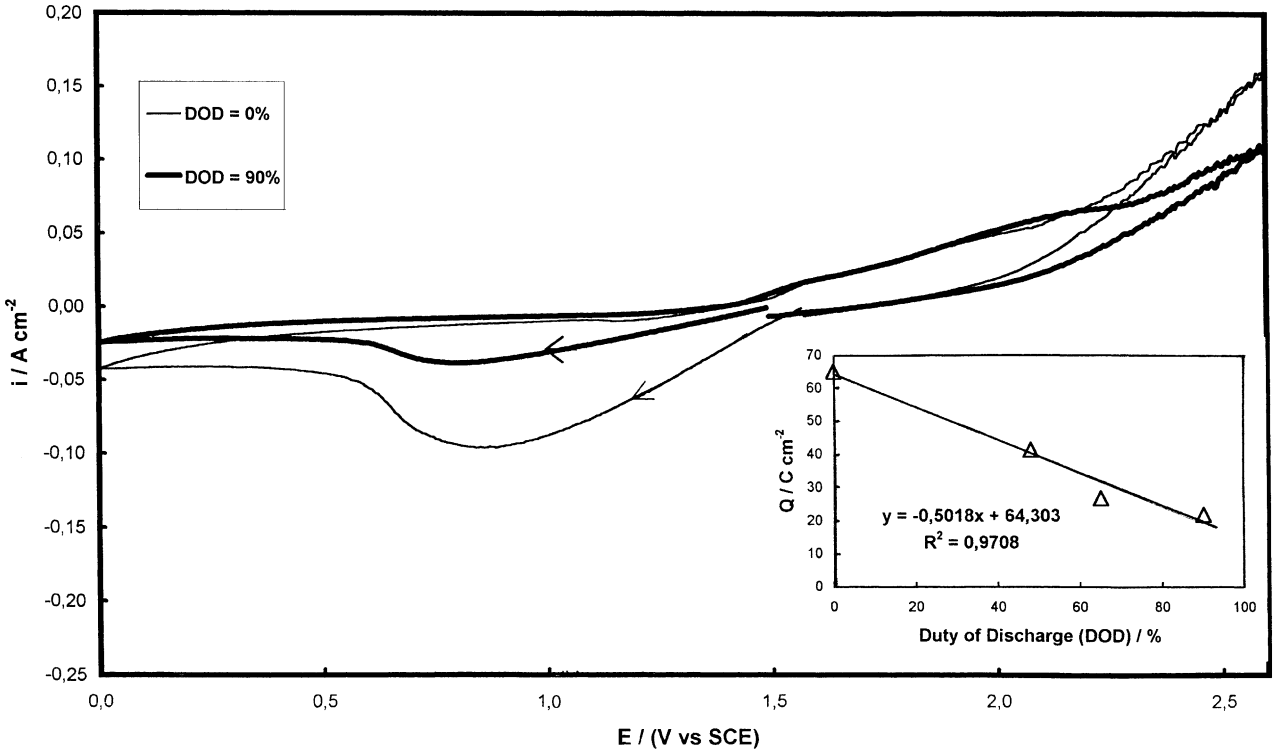

Fig. 5. Cyclic voltammograms at 1 mV s^{-1} potential sweep rate of positive plate specimens discharged at 0.085 A to 0 and 90% DOD levels. Inset: variation of the charge under the voltammogram cathodic peak with specimen DOD.

Finally, to correlate the remaining charge with the amount of active PbO_2 present after usage up to various DOD's the cyclic voltammetry of the specimens was recorded. Fig. 5 presents cyclic voltammograms of specimens of two indicative DOD's (0 and 90%), recorded in 5 M H_2SO_4 at a potential sweep rate of 1 mV s^{-1}, starting from the rest potential and going negative. The features of these voltammograms compare well with those for pure Pb [28], pre-anodised Pb [29] and other positive battery plate electrodes [30]. The wide cathodic peak between 1.5 and 0.5 V versus SCE corresponds to the (partial) reduction of PbO_2 to $PbSO_4$ whereas the anodic peak between 1.5 and 2.25 V versus SCE corresponds to the (partial) oxidation of $PbSO_4$ to PbO_2. The charge corresponding to the amount of remaining PbO_2 discharged during the cathodic scan of this potentiodynamic experiment was found from the area under the wide cathodic peak and is plotted for various prior DOD's in the inset of Fig. 5. Again, a smooth variation is observed.

Thus, the procedure adopted for obtaining specimens of different SOC's resulted in specimens whose DOD could be correlated to their SOC, expressed either as remaining charge or remaining PbO_2.

3.3. Electrochemical characterisation of state of charge of battery plate specimens by means of galvanostatic discharge using an electrode probe in contact mode

Fig. 6 shows the E versus t transients recorded under galvanostatic discharge at 0.085 A for a fully charged specimen (DOD = 0%), using either the cell of Fig. 1(a) (total discharge mode, solid line curve) or that of Fig. 1(b) (probe discharge mode, thick solid line curve). Two observations can be readily made: the initial voltage drop is much higher for the probe discharge experiments (close to 2 V compared with about 100 mV for the total discharge mode) but the time required for deep discharge and the voltage drop between the plateau and end potentials (2.08 and 2.1 V, respectively) is similar for both experiments. The latter indicates that, as also mentioned in Section 1, due to the porous nature of the specimen, its discharge via the small electrode probe enclosed in an insulating body and in contact with the sample finally results in the discharge of the entire specimen.

The initial voltage drop (within tens or a few hundred seconds) after the application of the constant current for both experiments is due to Ohmic losses (*IR* drop) in the acid solution and through the specimen and to the development of an overpotential (electron transfer and crystallization overpotential) for the $PbO_2 \rightarrow PbSO_4$ transformation. Both of these contributions are expected to be higher in the case of probe discharge since the current path passes through the small probe tip aperture (0.06 cm^2 area) and even a partial field localisation under the tip will result to a higher local current density and increase in local overpotential; hence, the voltage drop for the probe discharge is significantly higher.

The top inset of Fig. 6 shows in more detail the initial voltage drop during total discharge, ΔE_{in}, which is completed

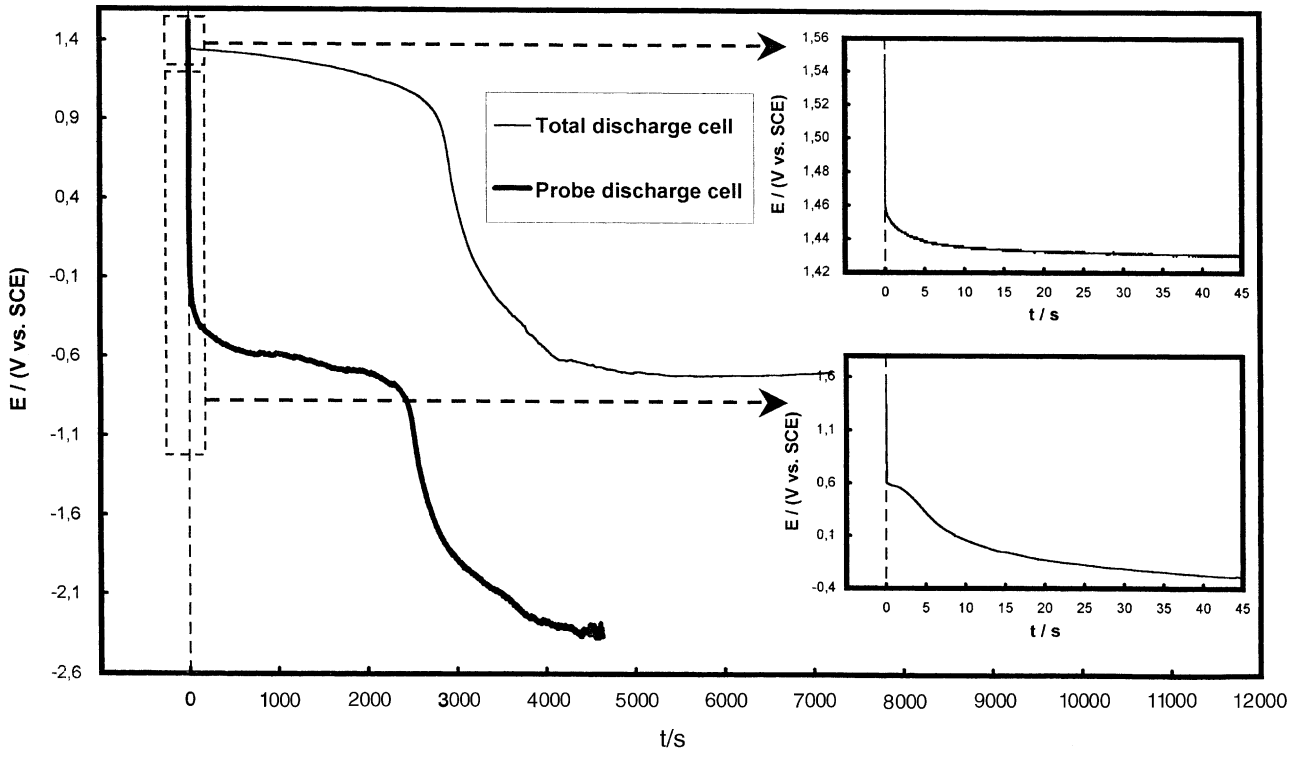

Fig. 6. Potential vs. time discharge curves during "total" (solid line curve) and "probe" (thick solid line curve) discharges at 0.085 A. Insets: details of initial potential decays.

within 10 s and has a magnitude of 0.110 V. This is in reasonable agreement with the value of 0.095 V estimated if we take into account the average specimen resistance of $R_{ave} = 1.11\ \Omega$ given in Section 3.1 and the discharge current of 0.085 A. The curve in the second inset shows the detail of the initial stages of probe discharge, revealing the existence of an additional feature: a hump or inclined plateau extending ca. 5 s. Thus, the initial voltage drop, which during the first 45 s is $\Delta E_{in} = 1.81$ V, is realised in two steps. The first one is instantaneous and corresponds to $(\Delta E_{in})_1 = 0.9$ V while the major part of the second one is realised within ca. 5 s and corresponds to $(\Delta E_{in})_1 = 0.86$ V after 45 s. It should be noted that the voltage fall in the case of probe discharge extends (although at a decreased rate) well beyond the 45 s shown in the inset (a plateau value is only achieved after some 500 s, see main part of Fig. 6).

At a first sight it would seem that this feature corresponds to the complete discharge of the area under the tip, before the discharge spreads through the porous specimen to the rest of the sample. This possibility is unlikely due to various reasons. First of all SEM micrographs of specimens discharged only for 10 s showed that there was no significant $PbSO_4$ crystal formation and no material segregation characteristic of deep discharge under the tip; more important, there were no noticeable differences between the area under the tip and the rest of the specimen surface. Second, if the initial discharge was fully concentrated on the small area under the probe (0.06 cm^2) this would correspond to a very high local current density (1.41 A cm^{-2}) which, if as a rough estimate we accept the validity of the linearised Peukert's equation given in Fig. 2(a) after its translation to current densities, gives a time of just 0.236 s for the completion of local discharge. Third, if the electric field is restricted to the specimen under the tip area only, then a crude estimate of the resistance through the 0.06 cm^2 of specimen, using the value of $R_{ave}A = 3.2\ \Omega\ cm^2$ found in Section 3.1, gives $R_{ave} = 53.33\ \Omega$, resulting in an initial voltage drop of $(\Delta E_{in})_1 = 4.53$ V which is higher than the 0.9 V observed. A more accurate calculation would take the acid resistance as the uncompensated solution resistance to a disc electrode corresponding to the tip aperture of radius $r = 0.14$ cm and in large distance from the reference and counter electrodes (equal to and larger than 1.2 cm in our case, see Fig. 1(b)) and given by [31]:

$$R_{acid} = \frac{1}{4\kappa r} \tag{4}$$

Therefore, $R_{acid} = 2.75\ \Omega$ and, since $R_{plate} = (R_{plate}A)/A = 1.35\ \Omega\ cm^2/0.06\ cm^2 = 22.5\ \Omega$ (as found in Section 3.1), it follows that $R_{ave} = R_{plate} + R_{acid} = 25.25\ \Omega$, resulting in an initial voltage drop of $(\Delta E_{in})_1 = 2.15$ V which is again higher than the 0.9 V observed. On the other hand, if we assume that the significant difference in the initial voltage drops between the total and probe discharge experiments is merely due to the restriction of the final aperture of the current path through the acid, whereas there is no

localization at all of the electric field through the specimen under the tip (i.e. if we assume that the entire specimen of 2.89 cm^2 discharges uniformly) then the value of $R_{plate} = (R_{plate}A)/A = 1.35\ \Omega\ cm^2/2.89\ cm^2 = 0.47\ \Omega$ has to be added to $R_{acid} = 2.75\ \Omega$ to give $R_{ave} = 3.22\ \Omega$, resulting in an initial voltage drop of $(\Delta E_{in})_1 = 0.27$ V which is smaller than the 0.9 V observed. Hence, neither complete discharge localization nor uniform discharge occurs. It seems that at least some partial localization of discharge occurs during the first stages of the probe discharge experiment. It could be that during the first stages of the probe discharge a thin film of insulating $PbSO_4$ is formed throughout the sample but preferentially under the tip (inclined plateau in the corresponding short time curve). When this film reaches a critical thickness or coverage (not visible in SEM micrographs) and the specimen electronic and ionic conductivity a critically small value (within ca. 5 s) then the discharge spreads/continues through the pores of the area under the tip gradually to the rest of the specimen, giving rise to the main plateau in the E versus t curve (notice also the ill-defined plateau in the long term discharge curve of the probe experiment in Fig. 6). In other words, this behaviour results from the interplay of Ohmic losses under the tip (increasing at higher rates since both the surface resistivity rapidly increases at the higher local current densities and the increase in local resistance is further accentuated due to the narrow current path cross-sectional area at the probe tip) and Ohmic losses at more remote locations on the specimen (where the current path is longer but its cross-sectional area higher and the rate of resistivity increase due to $PbSO_4$ formation lower).

Fig. 7 presents the short-term E versus t probe discharge curves of specimens of different DOD's. It can be seen that the instantaneous voltage drop increases significantly with DOD since the amount of $PbSO_4$ into which PbO_2 is transformed in discharged or partially discharged samples increases too. These results in a decrease of specimen electronic and ionic conductivity and hence an increase of Ohmic losses too, while the decrease in active PbO_2 surface results in an increase of current density and higher electron transfer overpotential. However, the exact determination of instantaneous voltage drop which could then be used as an indication of its SOC, would require the extrapolation of the E versus t curve to zero time, a procedure which unless done very carefully can lead to inaccurate results. On the other hand, there is a distinctive difference between fully charged specimens (DOD = 0%) and specimens as little discharged as those with a DOD = 25% with respect to the shape and duration of the short-term hump. In the former the hump is clearly visible and the inflection point of the corresponding S-shaped feature of the E versus t curve occurs at longer times (ca. 7 s, see curve derivative given in inset A) than

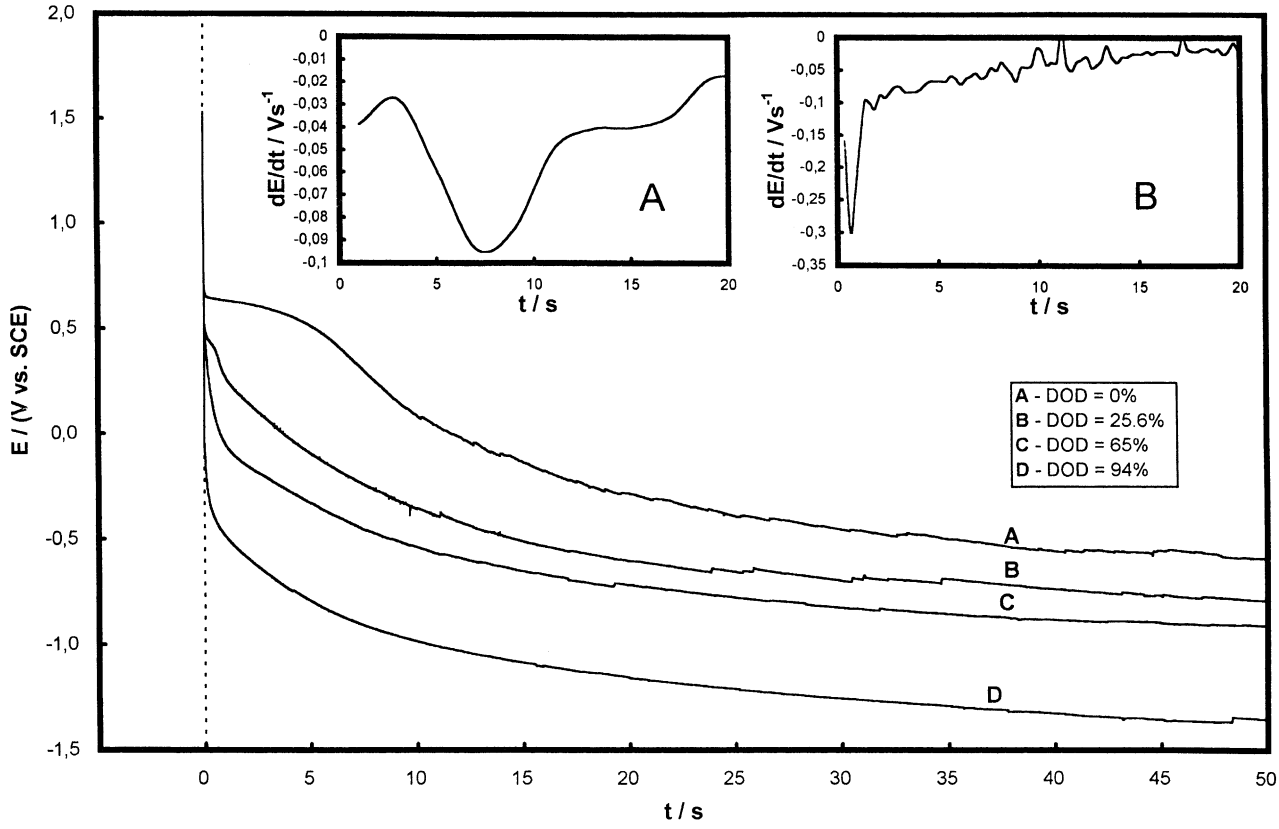

Fig. 7. Initial decay of potential vs. time discharge curves (A–D) during "probe" discharges at 0.085 A for various DOD values (A–D). Insets: first derivatives of curves A (0% DOD) and B (25.6% DOD).

those observed for the latter (ca. 0.65 s, see curve derivative given in inset B). For specimens with a DOD of 40% or above no such feature is observed. This is likely to be due to the fact that for these heavily discharged samples, the formation of the critical amount of discharge products and associated critical Ohmic losses under the tip (needed for the spread of the discharge to the entire specimen) have already taken place during their formation-prior discharge to the required DOD level.

It should be noted that similar results were obtained on positive plate specimens of another battery type (Hawker–Oldham EA13) too as well as in solutions of 3 and 1 M H_2SO_4 (where higher instantaneous Ohmic losses were observed but the hump was still present for fully charged specimens). The latter set of experiments proves that the hump is not associated in any way with sulphuric acid concentration but only with the SOC of the specimen and more important (for a possible in situ use of the technique, where the acid concentration drops at the same time as the DOD increases) that this feature is not present for discharged plates in dilute acid solutions.

4. Conclusions—future work

Discharging positive lead–acid battery specimens under galvanostatic control by firmly contacting on its surface the fine aperture tip of a small probe containing a counter and a reference electrode in an insulating glass body, gave rise to E versus t curves with some interesting features which are related to the SOC of the specimen. Apart from the increase in the spontaneous voltage drop with increasing DOD, the most interesting element of these E versus t transients is a consistently observed potential arrest before the attainment of the main potential plateau (observed in conventional discharge experiments) and well before the final voltage drop of deep discharge of the entire specimen. This potential arrest was particularly visible for fully charged specimens and its duration (<10 s for the battery specimens used) decreased with increasing DOD. Based on SEM results, local current density considerations, and resistance calculations, it follows that this feature is not due to complete discharge localisation under the probe tip but rather to the time needed for the film of $PbSO_4$ formed and the resistance under the tip both to reach a critical value for the discharge to spread to other locations of the sample. However, unlike the coulometric metal thickness gauge which stimulated the idea for a similar battery plate probe, the electric field finally spreads to the entire specimen due to the latter's porous nature and deep discharge of the entire specimen can be observed.

The prominence of this short-time potential arrest during probe discharge experiments of fully charged plate specimens and its gradual disappearance for partially discharged specimens can be used in the development of a battery plate production quality control procedure. Each plate could be rapidly tested in the production line by simply pressing a discharge probe on it and applying a galvanostatic pulse. Since the measurement is taken over a small plate area and, more important, during this short potential arrest no deep discharge is observed even under the probe's tip area, the method can be considered as non-destructive.

Although the application of the technique in battery plate quality control seems rather straightforward, its potential use for the development of an in situ battery SOC probe is more demanding and would require more research both into the fundamentals of the process and into probe design matters. First of all, a detailed correlation between battery DOD and the duration of the potential arrest (as quantified by the inflection point of the E versus t curve or a minimum of its derivative) has to be established as well as an understanding of its origin, e.g. by means of surface sensitive spectroscopic techniques. Second, miniaturisation of the probe and battery re-design will be needed for its incorporation in the battery body. With respect to the latter, a simple approach (currently used in crude battery tests in our laboratory) is to use a very thin Ag/AgCl reference and a fine Pt counter electrode cased in a glass capillary (1 mm i.d.). The capillary is bend at its end by 90° and sealed with a frit made of Vycor®. The probe is attached on a thin plastic frame inserted between the battery plate and the separator. Sliding of the frame and probe at different locations and pressing them on the battery plate during periodic testing is achieved by a finger-tight screw mechanism on the battery top and bottom parts. A second, more sophisticated approach, would be to print reference and counter electrodes at various locations on the surface of the battery separator with electrical connections made via miniature insulated wires through its body. Insulating plastic rings of say 1–2 mm diameter and say 1 mm depth could be fabricated around each electrode couple. These micro-probes could be kept pressed on the battery plate by appropriate sandwiching the separator between plates. We believe that the preliminary findings of the probe discharge experiments presented in this paper could set the foundations for the development of a cheap and simple in situ SOC probe.

Acknowledgements

P.J. Blood acknowledges the University of Nottingham Research Opportunity Fund scholarship.

References

[1] H. Bode, Lead–Acid Batteries, R.J. Brode, K.V. Kordesch (Translation), Wiley, New York, 1977.
[2] G. Smith, Storage Batteries, Pitman Publishing Ltd., London, 1980.
[3] K.V. Kordesch, Lead–Acid Batteries and Electric Vehicles, Marcel Dekker, New York, 1977.
[4] C.A. Vincent, B. Scrosati, Modern Batteries, 2nd Edition, Arnold, London, 1997.

[5] T.R. Crompton, Battery Reference Book, Butterworths-Heinemann, Oxford, 1997.
[6] A.J. Appleby, J. Power Sources 53 (1995) 187.
[7] W.G. Sunu, B.W. Burrows, J. Electrochem. Soc. 128 (1981) 1405.
[8] E. Hwang, J. Lee, M. Kim, J. Korean Chem. Soc. 36 (1992) 42.
[9] A. Eklund, F. Alavyoon, D. Simonsson, R.I. Karlsson, F.H. Bark, Electrochim. Acta 36 (1991) 1345.
[10] C.W. Chao, S.P. Lin, Y.Y. Wang, C.C. Wan, J.T. Yang, J. Power Sources 55 (1995) 243.
[11] S.T. Hung, D.C. Hopkins, C.R. Mosling, IEEE Trans. Ind. Electron. 40 (1993) 96.
[12] J.L. Weininger, J.L. Briant, J. Electrochem. Soc. 129 (11) (1982) 2409.
[13] S. Rodrigues, N. Munichandraiah, A.K. Shukla, J. Power Sources 87 (2000) 12.
[14] M.L. Gopikanth, S. Satyanarayana, J. Appl. Electrochem. 9 (1979) 369.
[15] V.V. Viswanathan, A.J. Salkind, J.J. Kelley, J.B. Ockerman, J. Appl. Electrochem. 25 (1995) 729.
[16] M. Kim, E. Hwang, J. Power Sources 64 (1997) 193.
[17] A.R. Willey, D.F. Kelsey, Anal. Chem. 30 (11) (1958) 1804.
[18] R.H. Lambert, D.J. Trevoy, J. Electrochem. Soc. 105 (1) (1958) 18.
[19] W.H. Boctor, S. Zhong, H.K. Liu, S.X. Dou, J. Power Sources 77 (1999) 56.
[20] A.K. Graham, Electroplating Engineering Handbook, 3rd Edition, Van Nostrand Reinhold, New York, 1971.
[21] Fischer website: http://fischergb.co.uk.
[22] C.V. D'Alkaine, M.A.S. dos Santos, J. Power Sources 30 (1990) 153.
[23] C.V. D'Alkaine, A. Carubelli, H.W. Fava, A.C. Sanhueza, J. Power Sources 53 (1995) 289.
[24] C.V. D'Alkaine, A. Carubelli, M.C. Lopes, J. Appl. Electrochem. 30 (2000) 585.
[25] P. Ruetschi, R.T. Angstadt, J. Electrochem. Soc. 111 (12) (1964) 1323.
[26] P. Ruetschi, J. Electrochem. Soc. 120 (3) (1973) 331.
[27] C.V. D'Alkaine, A. Carubelli, M.C. Lopes, J. Power Sources 64 (1997) 11.
[28] A. Czerwinksi, M. Zelazowska, J. Power Sources 64 (1997) 29.
[29] Z. Takehara, J. Power Sources 85 (2000) 29.
[30] R. Fitas, L. Zerroual, N. Chelali, B. Djellouli, J. Power Sources 64 (1997) 57.
[31] J. Newman, J. Electrochem. Soc. 113 (5) (1966) 501.